Size and Shape Characterization for Shot-Peening Impingement Models

Paul Mort, Langdon Feltner, Mark Gruninger and David Bahr

Purdue University Department of Materials Engineering, Center for Surface Engineering Enhancement (CSEE)

Abstract

Size and shape characterization of shot is used to develop an impingement model that accounts for the effect of impact momentum and radius of curvature at the point of peening impact. The model parameters include the shot particle's size-dependent mass, shape-dependent radius of curvature (ROC), and a probability function for ROC selection based on possible orientations of the shot particle. The ROC model is based on shape archetypes of cast and cut-wire shot which are calculated based on relatively simple features obtained from 2D dynamic image analysis.

Introduction

Recent advances in modeling compressive stress fields achieved by shot peening have used idealized shot particles impinging on a substrate, the latter described as a mesh of finite elements (Xiao, Tong, Li, Yang, & Gao, 2017) (Xiao, et al., 2018). Finite Element Analysis (FEA) enables the prediction of surface coverage, work flux, and stress-depth profiles in the substrate; all are of interest in the industrial shot-peening community. Models using multiple discrete impacts can be used to provide statistical information on the distributions of coverage and stress field (Miao, Larose, Perron, & Lévesque, 2009) (Ghelichi, Crispiatico, Guagliano, & Bagherifard, 2018). Critical to the accuracy of the FEA model is the descriptive features of the shot particle size and shape distributions, as shot particle momentum and radius of contact have been shown to have a direct and significant impact on the induced stress state below the impact (Meguid, Shagal, Stranart, & Daly, 1999) (Larour, Bäumer, Dahmen, & Bleck, 2013).

The motivation for the current work is to expand the capability of FEM modeling to include distributions in shot characteristics: size and shape. The result is a distribution of shot particle mass and local radius of curvature (ROC) at the point of peening impact; when implemented in FEM, this provides additional modes of coverage and stress field distribution on the target substrate.

Experimental

Characterization was done using Dynamic Image Analysis (DIA);[*] the method has developed into a mature technology for particle characterization, capable of measuring size and shape distributions of particles based on their 2D projections in flows that can be manipulated to promote either aligned or random orientation. Random orientation is chosen to provide a statistical analogy of peening impacts. Both cast and cut-wire samples were characterized, typically imaging more than about 10k particles per sample to achieve robust statistical datasets. Data were collected for four grades of cast shot (S70, S110, S230, S330),[†] and four grades of twice-conditioned cut-wire shot (CW12, CW14, CW20, CW32).[‡]

Raw data collection included grayscale images (0-255) on a back-lit white (255) background; the grayscale images are binarized using a threshold (173 was used in this work) and then analyzed to provide size and shape information for each particle in the dataset. This procedure is summarized in Figure 1. Thresholding and analysis can be done in real-time during a measurement, or can be done by post processing the raw image data. This provides an output list having the size and shape characteristics of each particle; the detailed list can be further reduced to provide statistical distributions of size and shape features.

[*] SolidSizer, JM Canty, Lockport, NY, USA and Dublin, Ireland
[†] Ervin Industries, Adrian, MI, USA
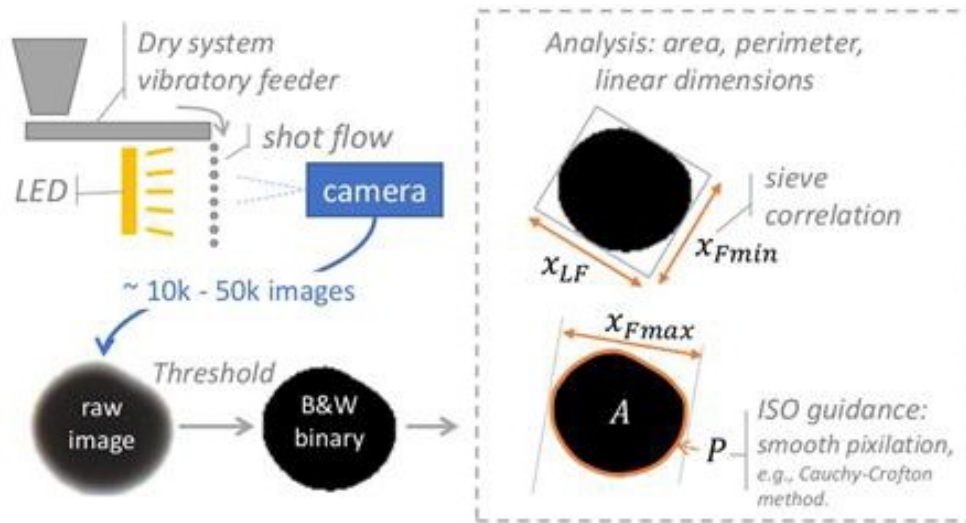[‡] Toyo Seiko NA, South Bend, IN, USA

Figure 1. Dynamic image analysis experimental setup, image thresholding, and feature analysis.

DIA features include 2D area (A), perimeter (P), min and max Feret lengths (x_{Fmin}, x_{Fmax}) and the orthogonal to the min Feret, x_{LF}. Feret lengths are linear dimensions between two parallel tangents. Shape factors derived based on these features are summarized in Table 1. The elliptical form factor is defined as an elliptical analogy of the ISO-defined form factor, where the factor β is used to approximate the perimeter of an ideal ellipse having an aspect ratio AR. The reduced curvature diameter is defined using the archetype for cast shot, which is based on overlapping or "glued spheres" (Figure 2).

Table 1. Summary of size features and shape factors obtained using dynamic image analysis

| Size Features	Impact curvatures & probabilities	Shape Factors (dimensionless)
• x_{Fmin} = min Feret length • x_{LF} = Feret length orthogonal to x_{Fmin} • x_{Fmax} = max Feret length • A = area • P = perimeter • x_A = equivalent area diameter, $x_A = \sqrt{4A/\pi}$ • V = volume, $\frac{4}{3}A^{3/2}/\sqrt{\pi}$	• x_{RC} = reduced curvature diameter, $\frac{-b+\sqrt{b^2-4ac}}{2a}$; $a = \frac{\pi-2}{8}$; $b = \frac{x_{Fmax}-x_{Fmin}}{2}$; $c = \frac{4 \cdot x_{Fmax} \cdot x_{Fmin}+(\pi-2)x_{Fmin}^2}{8} - A$ • $ROC1$ = major curvature $\sim x_{Fmin}/2$ • $ROC2$ = minor curvature $\sim x_{RC}/2$ • $d_{cc} = x_{Fmax} - (x_{Fmin} + x_{RC})/2$ • $\cos(\alpha) = (ROC1 - ROC2)/d_{cc}$ • $\Phi1$ = major probability, $(\pi - \alpha)/\pi$ • $\Phi2$ = minor probability, α/π	• AR_{ISO} = aspect ratio, ISO definition, x_{Fmin}/x_{Fmax} • AR_{box} = aspect ratio, bounding box, x_{Fmin}/x_{LF} • FF = form factor, $\frac{4\pi A}{P^2}$ • EFF = elliptical FF, $\frac{\beta\pi A}{P^2}$; $\beta = \left(\frac{1.5\cdot(AR+1)}{\sqrt{AR}} - 1\right)^2$
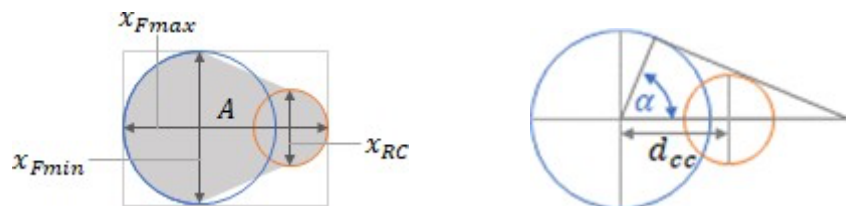
Figure 2. Archetype for reduced curvature: LHS) derivation of xRC; RHS) derivation of impact probability.

Results and Discussion, Characterization

Idealized archetypal particle shapes representing cut-wire and melt-atomization cast shot processes are shown on a shape map diagram (Fig. 3). The contour lines show parameters used to define the shapes. The shape map plots the Aspect Ratio and Elliptical Form Factors as orthogonal axes; the ordinate (AR) showing elongation, and the abscissa (EFF) showing angularity or other perimeter irregularity. In both cases, a value of (1,1) represents a circular projection of an ideal sphere.
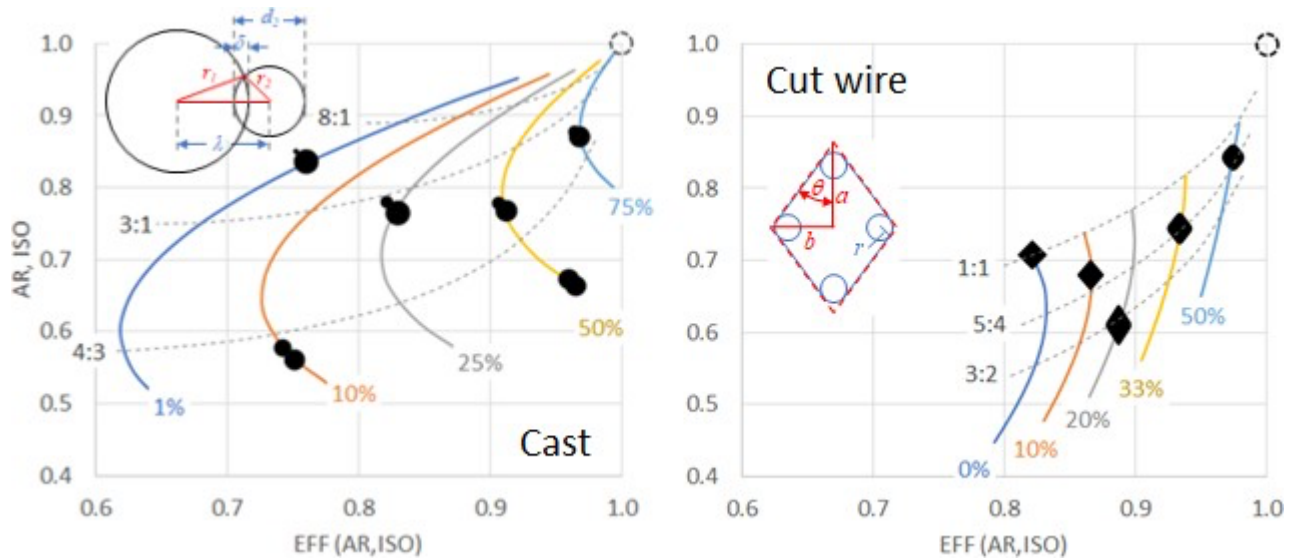

Figure 3. Shape mapping using conditioned cut-wire and atomized cast w/ satellites. Cast: colored contours represent the overlap of satellites; dashed contours represent their size ratio. Cut wire: colored contours refer to relative rounding of cut corners, r/b; dashed contours refer to cut orientation, a/b.

An example of shape mapping with experimental data is shown in Figure 4. The mapped particles are illustrated by their DIA images. Most of the particles (~90%) have a Form Factor that is > 0.95, i.e., highly spherical. The tail of the distribution has the more irregular shapes shown on the map.
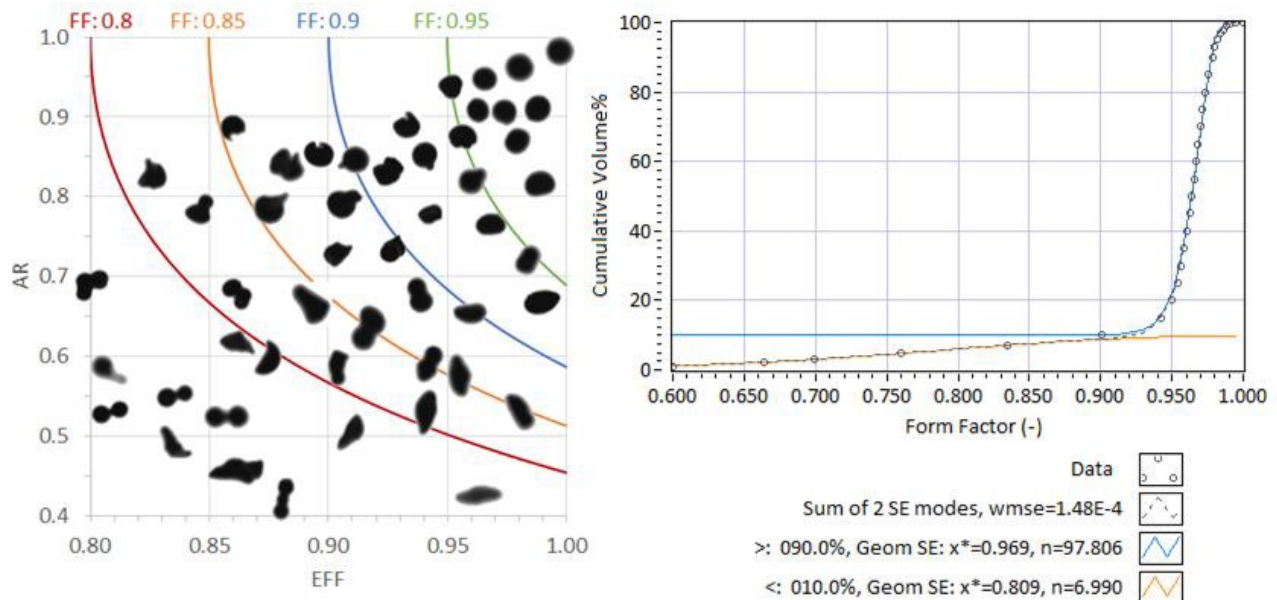

Figure 4. Shape mapping and distribution statistics for S70 shot.

Results and Discussion, Impact Modeling

The effect of the shape curvature analysis broadens the distributions of impact curvature versus conventional spherical shape assumptions (Figure 5). This is further illustrated in Figure 6, comparing a spherical assumption (black) with a glued-sphere representation.
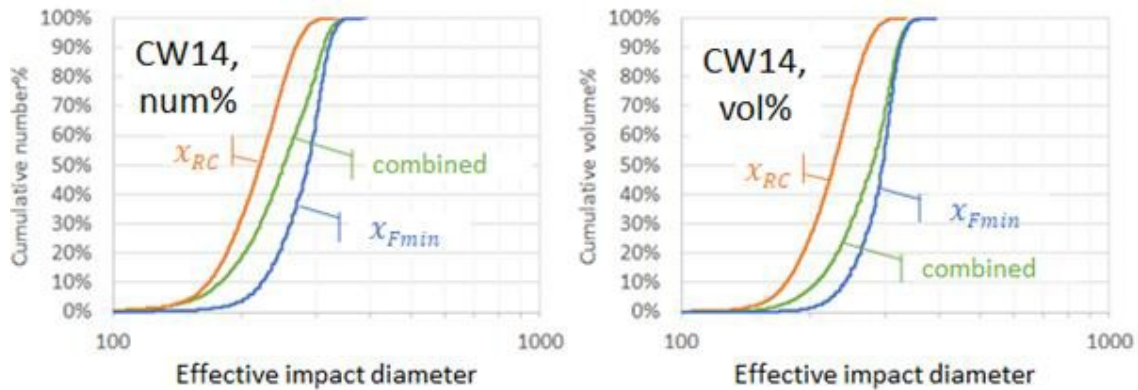
Figure 5. Effective impact curvature distribution for a cut-wire sample.

Combined (x_{Fmin}, x_{RC}) size distributions were created as inputs to a set of discrete-impact FEM models. These were compared to spherical equivalent models without shape effects, using the stress depth profile as a means of comparison. An Abaqus input file generation script was created that reads image data from the Canty SolidSizer imaging system. From this, area equivalent diameter and reduced radius of curvature are calculated for each particle in the distribution. From a user specified coverage percentage and shot size, an approximate number of impacts needed to reach the desired coverage is calculated.
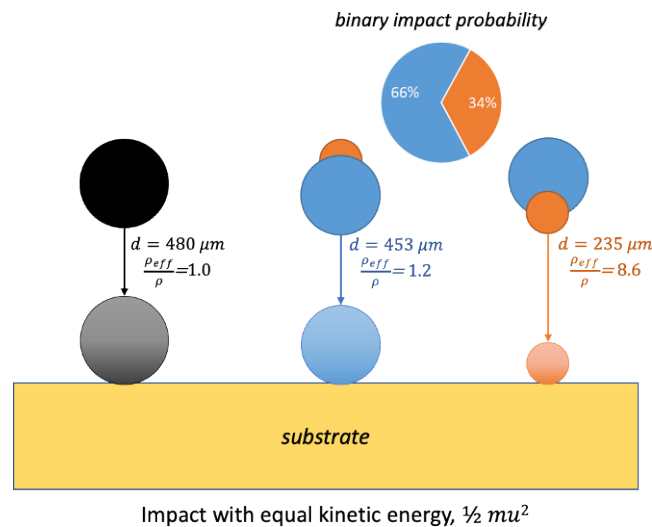
Figure 6. Area equivalent diameter (black) and glued sphere (orange and blue) representation of shot particles. Glued spheres have a smaller radius of contact with the same mass, translating to a higher effective density upon impact.

With each run of the input file generator, the number of necessary particles is sampled from the distribution and placed in random locations above the substrate. Each particle is assigned a radius of contact, based either on the area equivalent diameter (Fig 6, black), or a weighted probability of impacting with either $ROC1$ (Fig 6, blue) or $ROC2$ (Fig 6, orange). Mass was assigned to all particles based on the area equivalent diameter and the material density, ρ.
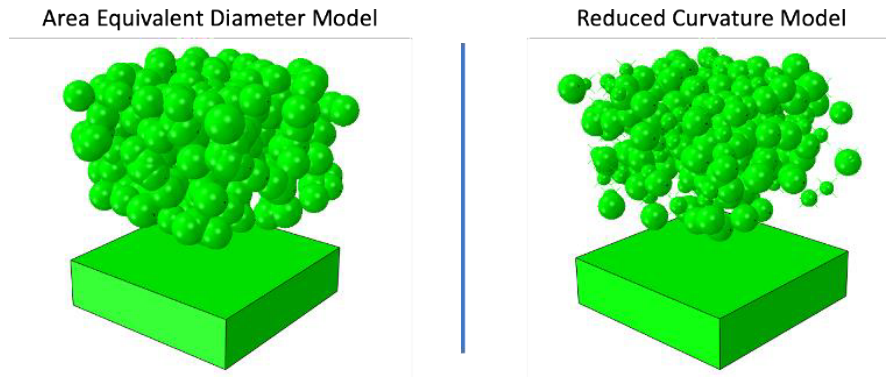
Figure 7. Area equivalent diameter representations of shot particles have a larger radius of contact for particles with similar mass.

A 5mm x 5mm representation of an Almen strip was used as the substrate, utilizing Johnson-Cook plasticity. Particles were not allowed to interact with each other, and all impacts were normal to the substrate surface at 65 m/s. As is shown in Figure 7, particles defined by area equivalent diameter have a larger radius of contact for particles of a similar mass. This means that there is a higher effective density multiplier for each of the smaller particle representations in the reduced curvature model.

This difference in effective density of particles translates to differences in both coverage/surface roughness and induced stress state in the substrate. As shown in Figure 8, the reduced curvature radius of contact definition tends to have deeper dimples with smaller radii, whereas the area equivalent dimples seem to be more evenly distributed in size and depth. By virtue of this, the area equivalent diameter seems to have a more uniform coverage, with less bare area (dark blue, Figure 8) where no particles have contacted.
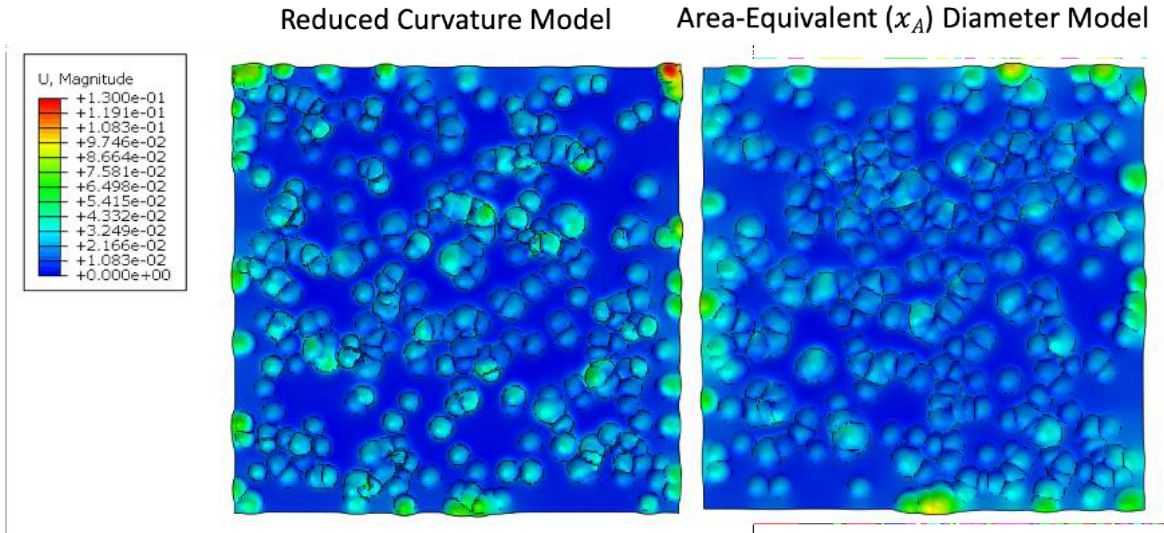

Figure 8. Deformed substrates with magnitude of displacement of surface nodes shown as the color gradient.

The differences between the particle radius of contact definitions are also shown in the induced stress-depth profiles through the thickness of the substrates. In both the 312 (~100 percent theoretical coverage) and the 937 (~300 percent coverage) trials, the area equivalent radius of contact definition produces a deeper cross over depth. Coupled with a similar peak stress and surface stress for both trials, this means that the area equivalent diameter particle definition translates to more cumulative work done on the substrate. Both trials have similar kinetic energies, only varying based on random sampling of the particle size distribution, and it can be inferred that there is more energy lost in the reduced curvature trials. Additionally, the curves show

that the reduced curvature radius of contact definition is less sensitive to number of impacts since there is a relatively small difference in cross over depth between the 312 and 937 impact trials in comparison to the area equivalent radius of contact definitions.
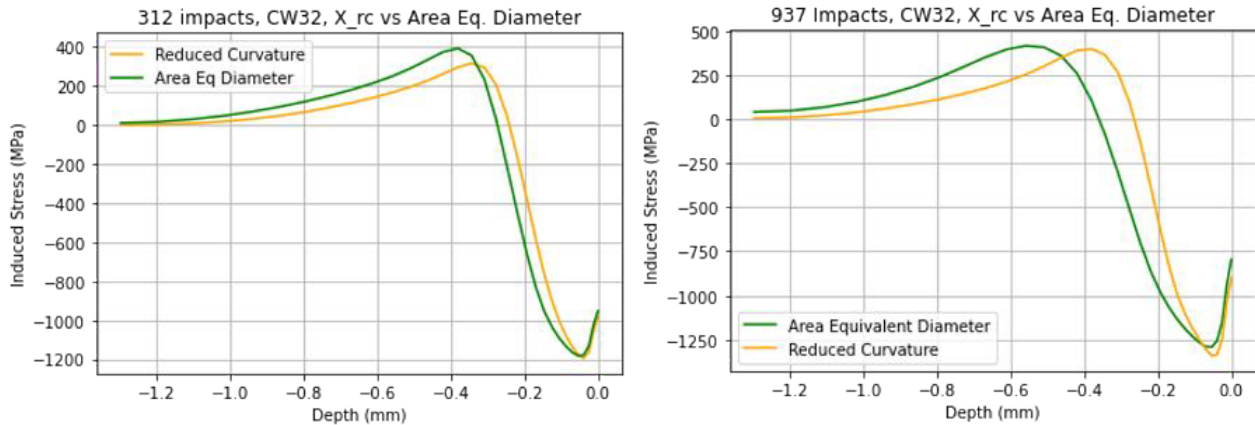

Figure 9. Induced stress states by way of area equivalent diameter and reduced curvature contact definitions in identical substrates, controlled for the number of impacts and impact velocity.

Conclusion

Measurement and analysis of shot media size and shape characteristics are of critical importance for model development. Media size and shape distributions affect surface coverage, work flux, and stress-depth profiles, all of which are of interest in the industrial shot-peening community. Both momentum of a particle and it's local radius of contact play a significant role in the formation of the induced stress state beneath it. Dynamic image analysis of shot media was used to develop an impingement model that accounts for the effect of impact energy and radius of curvature at the point of peening impact. Model parameters include the shot particle's size-dependent mass, shape-dependent radius of curvature (ROC), and a probability function for ROC selection based on possible orientations of the shot particle. Comparing finite element simulations having combined (x_{Fmin}, x_{RC}) radius of contact distribution versus an area-equivalent radius of contact, it is shown that the shape-dependent radius of contact has higher variability in local coverage and dimple size, and a reduced stress-depth profile. This means that non-spherical shapes reduce the work efficiency of the peening process. Future work will statistically quantify variability and work efficiency, and assess the effect of "working-mix" dynamics (i.e., media classification and recycle) in the peening process.

References

Ghelichi, R., Crispiatico, G., Guagliano, M., & Bagherifard, S. (2018). An energetic approach to predict the effect of shot peening-based surface treatments. *Metals*.

Larour, P., Bäumer, A., Dahmen, K., & Bleck, W. (2013). Influence of strain rate, temperature, plastic strain, and microstructure on the strain rate sensitivity of automotive sheet steels. *Steel Research International*, 426-442.

Meguid, S. A., Shagal, G., Stranart, J. C., & Daly, J. (1999). Three-dimensional dynamic finite element analysis of shot-peening induced residual stresses. *Finite Elements in Analysis and Design*, 179-191.

Miao, H. Y., Larose, S., Perron, C., & Lévesque, M. (2009). On the potential applications of a 3D random finite element model for the simulation of shot peening. *Advances in Engineering Software*, 1023-1038.

Xiao, X., Tong, X., Li, Y., Yang, M., & Gao, G. (2017). Numerical Research on the Effect of Boundary Constraint in Shot Peen Forming. *Journal of Materials Engineering and Performance*, 3839-3853.

Xiao, X., Tong, X., Liu, Y., Zhao, R., Gao, G., & Li, Y. (2018). Prediction of shot peen forming effects with single and repeated impacts. *International Journal of Mechanical Sciences*, 182-194.